Time-Resolved Resonance Raman and Density Functional Study of an Azirine Intermediate in the 2-Fluorenylnitrene Ring-Expansion Reaction To Form a Dehydroazepine Product

Shing Yau Ong, Peizhi Zhu, King Hung Leung, and David Lee Phillips*[a]

Abstract: We report time-resolved resonance Raman spectra for the azirine intermediate produced in the 2-fluorenylnitrene ring-expansion reaction to form a dehydroazepine product. The Raman bands obtained with a 252.7 nm probe wavelength and 500 ns delay time exhibit reasonable agreement with predicted vibrational frequencies from density functional calculations for two isomers of azirine intermediates that may be formed from a 2-fluorenylnitrene precursor. The Raman bands observed for delay times of 15 ns and 10 μs were consistent with predicted vibrational frequencies from density functional calculations for the 2-fluorenylnitrene and dehydroazepine product species as well as previously reported 416 nm time-resolved Raman spectra obtained on the ns and μs time scales. Our results demonstrate that the 2-fluorenylnitrene ring-expansion reaction to produce dehydroazepine products proceeds via relatively long-lived 2-fluorenylnitrene and azirine intermediates. Substitution of a phenyl ring *para* to the nitrene group of phenylnitrene appears to lead to significant changes in the ring-expansion reaction so that longer lived arylnitrene and azirine intermediates can be observed. This should enable the chemical reactivity of azirine intermediates formed from arylnitrenes to be examined more readily.

Keywords: arylnitrenes · azirines · density functional calculations · dehydroazepines · Raman spectroscopy

Introduction

The photochemistry of aryl azides[1–59] has been extensively investigated over many years by numerous research groups. The use of laser flash photolysis methods that directly probe the reaction intermediates and photoproducts has led to an increased understanding of their reaction mechanisms and intermediates. Solution-phase photolysis of aryl azides usually gives a singlet nitrene intermediate and a nitrogen molecule. The singlet nitrene intermediate can then undergo a fast ring-expansion reaction to form ketenimines (dehydroazepine) that can be readily trapped by nucleophiles. However, there are examples, such as the singlet 2-pyrimidylnitrene,[55] in which the singlet nitrene species mostly decays by intersystem crossing (ISC) to the triplet nitrene species. Triplet state arylnitrenes can subsequently form diazo products in some cases.

The reaction mechanisms and photochemistry of the prototypical singlet phenyl nitrene has been particularly well examined.[7, 8, 18, 20, 21, 42–46, 52–54] The singlet phenyl nitrene species has been directly seen in room-temperature solutions[44, 45] and was found to have a short lifetime of $\approx$1 ns. This is mainly the result of a fast ring-expansion reaction. A number of different substituents have been observed to significantly increase the lifetime of the singlet nitrene species.[16–18, 22–25, 29, 40, 55, 57] The photolysis of polyfluorinated phenyl azides in acetonitrile solutions formed singlet nitrenes with lifetimes of tens to hundreds of nanoseconds[40] because the substituents cause the ring-expansion reaction to have a higher activation barrier and proceed more slowly.[16–18, 22–25, 29, 40, 55, 57] These longer lived singlet nitrene species can be more readily trapped by nucleophiles (such as diethylamine, pyridine, and tetramethylethylene) and some have also been observed to form singlet arylnitrenium ions from a fast protonation reaction.[26, 28, 31–37, 40, 47, 48] Although much is known about the chemistry and reaction mechanisms of arylnitrenes, there are few direct vibrational mode-specific characterizations of singlet or triplet arylnitrenes in room-temperature solutions in the literature.

We recently reported a time-resolved resonance Raman spectroscopic study of arylnitrenes formed after ultraviolet photolysis of 2-azidofluorene in acetonitrile solution.[60] We observed a number of vibrational bands for two species and their vibrational frequencies were found to have reasonable agreement with those predicted from density functional

[a] Prof. Dr. D. L. Phillips, S. Y. Ong, P. Zhu, Dr. K. H. Leung
Department of Chemistry, The University of Hong Kong
Pokfulam Road, Hong Kong S.A.R. (P. R. China)
Fax: (+852) 2857-1586
E-mail: phillips@hkucc.hku.hk

Supporting information for this article is available on the WWW under http://www.chemeuj.org or from the author.

  0947-6539/03/0906-1377 $ 20.00+.50/0

calculations for singlet (and triplet) 2-fluorenylnitrene and their two ring-expansion dehydroazepine products, respectively.[60] The time-resolved resonance Raman bands of the 2-fluorenylnitrene species were observed to decrease in intensity with no prompt production of another intermediate or the dehydroazepine product seen in the 5 and 10 μs spectra.[60] This suggests there is an unobserved intermediate that is dark with respect to the 416 nm probe wavelength used in these time-resolved experiments. Since this unobserved intermediate is produced from the decay of the 2-fluorenylnitrene species and then subsequently forms the dehydroazepine products, it was suggested that the unobserved species could be a relatively long-lived azirine intermediate. Several other azirine intermediates have been observed in elegant matrix isolation experiments by Morawietz and Sander.[38] They were found to have a noticeable absorption band with a maximum ≈250 nm with little absorption in the 350–450 nm region[38] near the 416 nm used in our initial time-resolved resonance Raman study.[60]

Herein, we present a time-resolved resonance Raman investigation that used a 252.7 nm probe wavelength to attempt to observe the intermediate species not seen with the 416 nm probe wavelength. At a delay of 500 ns between the pump and probe pulses, we obtained a time-resolved resonance Raman spectrum whose vibrational frequencies are in reasonable agreement with those predicted for two azirine intermediates that could be formed from a singlet 2-fluorenylnitrene species. At 15 ns and 10 μs, different spectra were obtained and their vibrational frequencies are reasonably consistent with those predicted from density functional calculations for the singlet 2-fluorenylnitrene and the dehydroazepine products of 2-fluorenylnitrene, respectively. The 252.7 nm probe wavelength results correlate well with those obtained with the 416 nm excitation and demonstrate that the 2-fluorenylnitrene species decays to produce a fairly long-lived azirine intermediate that then proceeds to form the dehydroazepine intermediates observed in the 5 and 10 μs 416 nm time-resolved Raman spectra. To our knowledge, this is the first direct experimental structural evidence that an arylnitrene ring-expansion reaction proceeds via an azirine intermediate in room-temperature solutions. The *para*-substituted phenyl group in the fluorene moiety appears to significantly alter the relative stabilities of the nitrene, azirine, and dehydroazepine intermediates so that the ring-expansion reaction proceeds via a longer lived azirine intermediate. We briefly discuss the possibility of the use of nucleophiles and electrophiles to trap the longer lived 2-fluorenylnitrene and azirine intermediates in order to learn more about the chemical reactivity of these interesting reactive species.

Results and Discussion

Figure 1 presents the 252.7 nm time-resolved resonance Raman spectra obtained at 15 ns, 500 ns, and 10 μs after

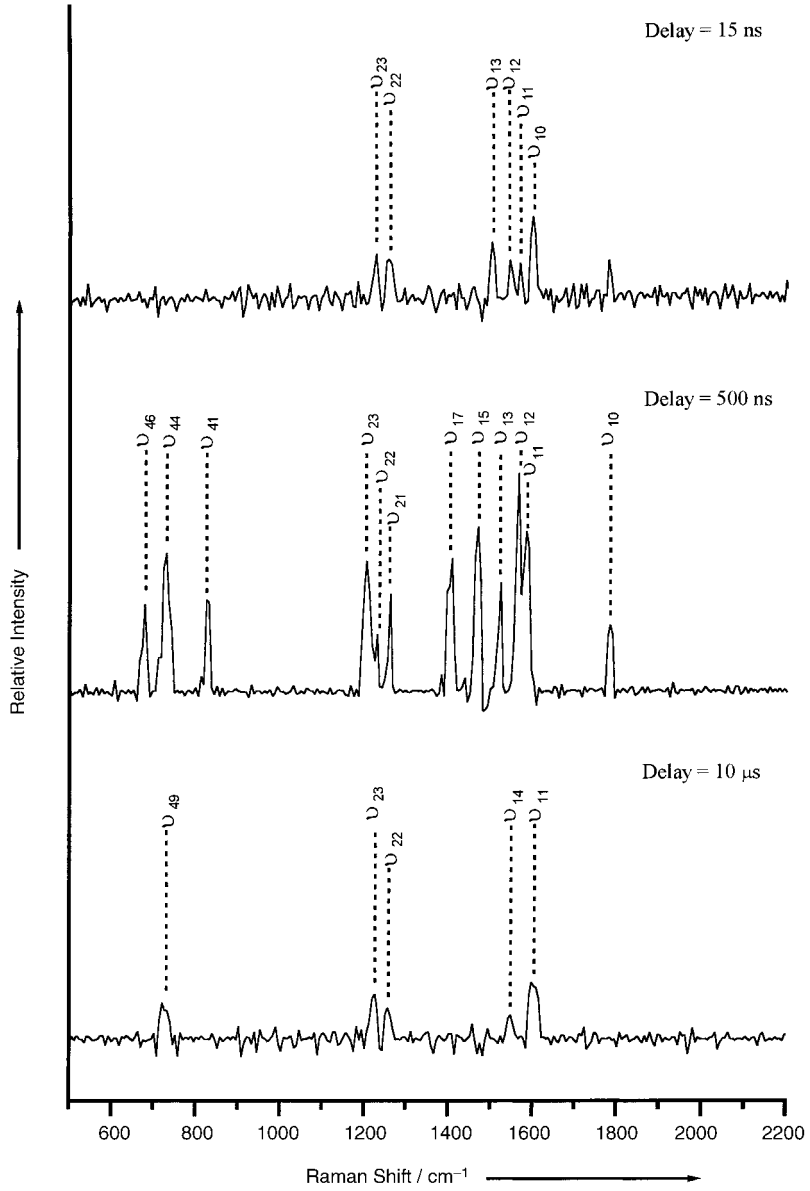

Figure 1. Time-resolved resonance Raman spectra acquired with 15 ns (top), 500 ns (middle), and 10 μs (bottom) time delay between the 309 nm pump and 252.7 nm probe laser pulses following photolysis of 2-azidofluorene in acetonitrile solution. The time-resolved resonance Raman spectra were found by subtracting the probe-only spectra and pump-only spectra from pump–probe spectra in order to remove solvent and precursor Raman bands. The larger Raman bands are labeled with their tentative assignments (see text and Tables 1, 2, and 3 for more details).

0947-6539/03/0906-1378 $ 20.00+.50/0 *Chem. Eur. J.* **2003**, *9*, No. 6

photolysis of 2-azidofluorene at 309 nm in acetonitrile. The 500 ns time-resolved resonance Raman spectrum is noticeably stronger than the spectra obtained at 15 ns and 10 μs. This suggests that the species observed at 500 ns is more resonantly enhanced with a 252.7 nm probe wavelength than the species observed at 15 ns and 10 μs. Use of a 416 nm probe wavelength in previous time-resolved resonance Raman experiments showed spectra of 2-fluorenylnitrene being stronger at 10 ns and decaying noticeably in the 50 ns and 100 ns spectra and almost gone in the 500 ns spectrum with no other apparent species being formed. The intermediate mainly present at 500 ns is easily observed with a 252.7 nm probe wavelength and difficult to observe with a 416 nm probe wavelength. This is consistent with results for several azirine intermediates which showed an absorption band with a maximum at ≈250 nm, but with little absorption in the 350–450 nm region in matrix isolation experiments.[38] Several investigations have used a comparison of DFT-computed vibrational frequencies to experimental values from either time-resolved Raman or IR spectra to assign several different arylnitrenium ions to their singlet ground states.[48, 56, 61, 62] We anticipate a similar approach should prove useful for nitrene, azirine, and dehydroazepine species.

We have performed UBPW91/cc-PVDZ computations to obtain the optimized geometry and predict vibrational frequencies for the two azirine isomers (**AZ1** and **AZ2**) that can be formed from the singlet 2-fluorenylnitrene species. The optimized geometry parameters found from the UBPW91/cc-PVDZ are listed in the Supporting Information. Figure 2 displays selected parameters from the UBPW91/cc-PVDZ calculations. Table 1 compares the UBPW91/cc-PVDZ computed vibrational frequencies and normal Raman intensities to the 500 ns time-resolved resonance Raman experimental values. Inspection of Table 1 shows that there is reasonable agreement between the calculated and experimental vibrational frequencies with differences of 16 cm^{-1} (for **AZ1**) and 17 cm^{-1} (for **AZ2**), on average, for the UBPW91/cc-PVDZ calculations. The twelve Raman bands observed in the 500 ns spectrum of Figure 1 cannot clearly distinguish between the two azirine isomers (**AZ1** and **AZ2**); however, the experimental vibrational frequencies are consistent with an azirine intermediate. In particular, the observation of the 1782 cm^{-1} Raman band in the 500 ns spectrum of Figure 1 is characteristic of the C=N stretch of the three-membered ring in azirines and similar to the 1708 cm^{-1} and 1730 cm^{-1} infrared vibrational bands observed for two azirines formed from the photolysis of 1-napthylazide in low-temperature matrix isolation experiments.[63] Therefore, we assign the 500 ns time-resolved resonance Raman spectrum obtained with a 252.7 nm probe wavelength to the azirine species formed from the 2-fluorenylnitrene precursor.

Inspection of Table 1 reveals that the computed normal Raman intensities are reasonably consistent with the resonance Raman intensities of the azirine intermediate observed at 500 ns for the higher frequency modes in the 1200–1800 cm^{-1} region. We note the caveat that the resonance enhancement of the Raman intensities can lead the intensity pattern to be substantially different in the resonance Raman spectrum compared to the normal Raman spectrum and this probably accounts for differences between the computed and experimental intensities. Several azirine intermediates in matrix isolation experiments have their most intense absorption band in the UV/Vis region around 250 nm, but little absorption in the 350–450 nm region.[38] The large oscillator strength of the 250 nm absorption band and little intensity in absorption bands at longer wavelengths suggests that the 250 nm band could make a substantial contribution to the nonresonant Raman spectrum and lead to some similarities in the Raman intensity patterns for the 250 nm resonance Raman and normal Raman spectra.

Comparison of the computed Raman vibrational frequencies and intensities to those of the experimental 500 ns TR^3 spectrum in Table 1 suggests that both azirine isomers (**AZ1** and **AZ2**) contribute to the experimental spectra. The experimental 500 ns TR^3 spectrum has intense Raman bands at 1408, 1469, 1523, 1566, and 1584 cm^{-1} bands in the 1370–1650 cm^{-1} region. Neither **AZ1** nor **AZ2** is predicted to have a large amount of intensity in modes correlating to all these bands. However, the presence of both **AZ1** and **AZ2** in noticeable amounts can account for a large degree of intensity in all of the 1408, 1469, 1523, 1566, and 1584 cm^{-1} bands of the experimental spectrum. The 1408 cm^{-1} experimental band can be assigned mainly to the **AZ2** ν_{18} mode (calculated to be at 1377 cm^{-1} with a Raman intensity of 140) with smaller contributions from the **AZ1** ν_{18} and/or ν_{17} modes. The 1469 cm^{-1} experimental band can be assigned mainly to the **AZ2** ν_{15} and/or ν_{16} modes (calculated to be at 1440 and 1454 cm^{-1} with intensities of 120 and 77 respectively) with smaller contributions from the **AZ1** ν_{15} and/or ν_{16} modes. The 1523 cm^{-1} experimental band can be assigned to both the **AZ2** ν_{13} mode (calculated to be at 1534 cm^{-1} with an intensity of 126) and the **AZ1** ν_{14} mode (calculated to be at 1517 cm^{-1} with an intensity of 220). The 1566 cm^{-1} experimental band can be mainly attributed to the **AZ1** ν_{13} and ν_{12} modes (calculated to be at 1583 and 1589 cm^{-1} with intensities of 125 and 193, respectively) and maybe some small contribution from the **AZ2** ν_{12} mode. The experimental 1584 cm^{-1} band can be assigned to both the **AZ1** ν_{11} mode (calculated to be at 1612 cm^{-1} with an intensity of 255) and the **AZ2** ν_{11} mode (calculated to be at 1614 cm^{-1} with an intensity of 222). The presence of appreciable amounts of both **AZ1** and **AZ2** intermediates can account for the experimental bands at 1408, 1469, 1523, 1566, and 1584 cm^{-1}, all having a large intensity and is reasonably consistent with the computed Raman intensities of the **AZ1** and **AZ2** species.

Based on our previous 416 nm time-resolved resonance Raman study,[60] we would tentatively assign the 252.7 nm 15 ns and 10 μs spectra in Figure 1 to the singlet 2-fluorenylnitrene and its dehydroazepine products (**DA1** and **DA2**), respectively. Tables 2 and 3 compare the Raman vibrational frequencies observed in the 252.7 nm 15 ns and 10 μs spectra in Figure 1 to the (U)BPW91/cc-PVDZ-computed vibrational frequencies for singlet 2-fluorenylnitrene and its dehydroazepine products (**DA1** and **DA2**). The six Raman bands observed in the 252.7 nm spectrum at 15 ns are in reasonable agreement with the calculated results. Different Raman bands are resonantly enhanced in the 252.7 nm spectrum compared to the 416 nm spectrum since the excitation wavelength is in

  0947-6539/03/0906-1379 $ 20.00+.50/0

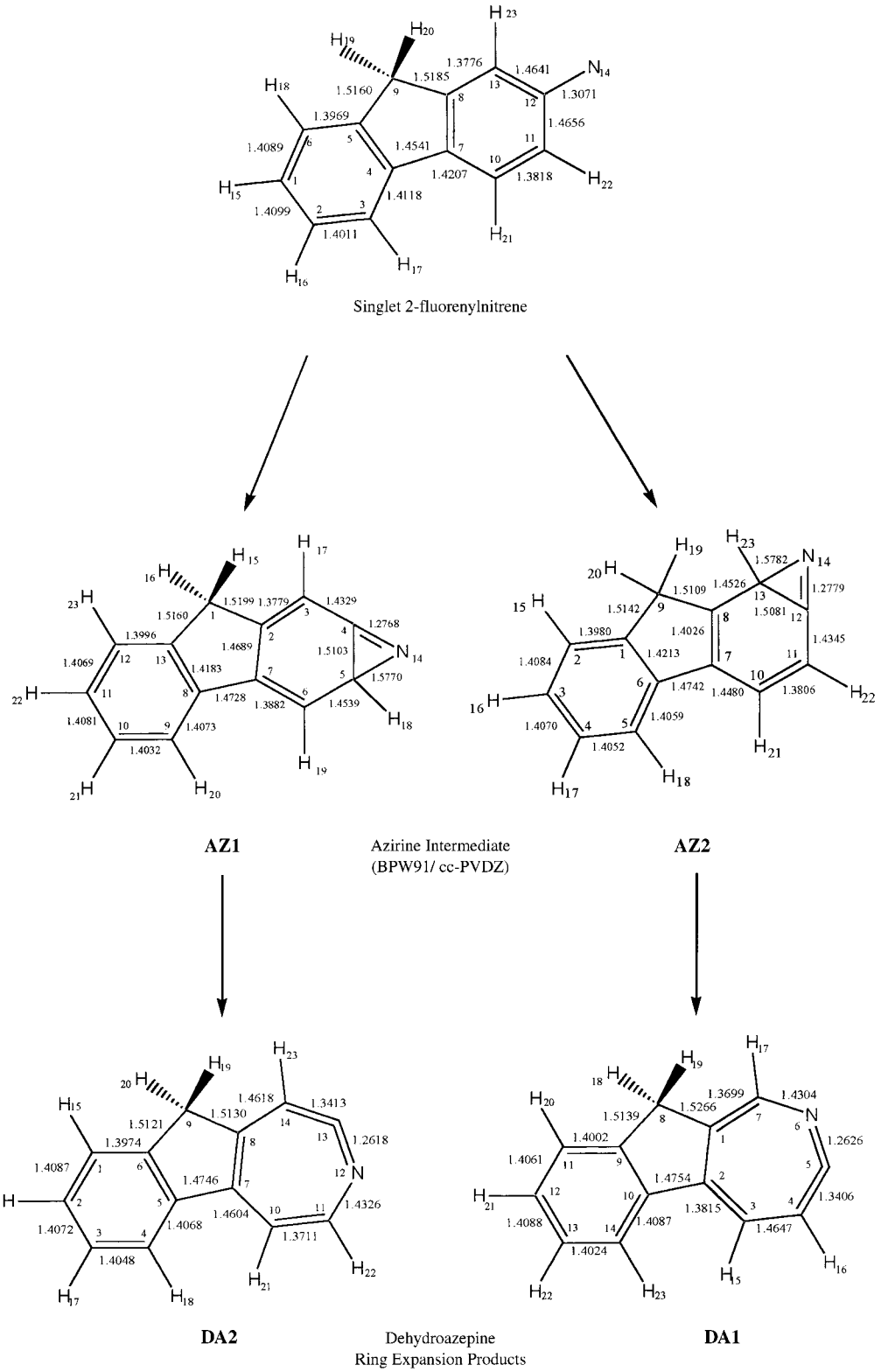

Figure 2. Schematic diagrams of the singlet state of 2-fluorenylnitrene, the two isomers of the azirine intermediates (**AZ1** and **AZ2**), and the two dehydroazepine product species (**DA1** and **DA2**) with the atoms numbered. The numbering of the atoms corresponds to those used in the Supporting Information of reference [60] for the UBPW91/cc-PVDZ and BPW91/cc-PVDZ calculations for the 2-fluorenylnitrene and dehydroazepine species (**DA1** and **DA2**) and the Supporting Information of this paper for the two azirine species (**AZ1** and **AZ2**). Selected geometry parameters (bond lengths [Å] and bond angles [°]) are shown in the diagrams.

resonance with different excited electronic states. The three bands in the C–C stretch region (ν_{10}, ν_{11}, and ν_{12}) are observed in both the 252.7 nm and 416 nm spectra. Their experimental frequencies are within 7 cm^{-1} of each other and consistent with being from the same 2-fluorenylnitrene species (note the mutual experimental uncertainty is

0947-6539/03/0906-1380 $ 20.00+.50/0 *Chem. Eur. J.* **2003**, *9*, No. 6

Table 1. Experimental Raman vibrational frequencies observed in the time-resolved resonance Raman spectrum at 500 ns shown in Figures 1 and 2.[a] The experimental vibrational frequencies are compared to those from BPW91/cc-PVDZ computations for the two isomers of the azirine intermediates formed from the decay of the 2-fluorenylnitrene species (see text for more details).

Azirine isomer 1 (**AZ1**)			Azirine isomer 2 (**AZ2**)			Experiment	
vibrational mode possible description	UBPW91/cc-PVDZ calcd freq. [cm^{-1}]	int. [arb. unit]	vibrational mode possible description	cc-PVDZ calcd freq. [cm^{-1}]	int. [arb. unit]	500 ns TR3 freq. [cm^{-1}]	int. [arb. unit]
ν_{49}, C + N + C bend	601	4					
ν_{48}, ring def.	619	2	ν_{48}, CCC bend	625	7		
ν_{47}, ring def.	649	4	ν_{47}, ring def.	632	6		
ν_{46}, CCC bend	**704**	**7**	ν_{46}, ring def.	689	1		
ν_{45}, ring def.	714	3	**ν_{45}, CCC bend**	**704**	**10**	**680**	**137**
ν_{44}, ring def.	**728**	**6**	**ν_{44}, C–H bend**	**724**	**2**	**729**	**209**
ν_{43}, ring def. + C–H bend	756	4	ν_{43}, C–H bend	763	4		
ν_{42}, CCC bend + C–H bend	773	20	ν_{42}, ring def.	780	5		
ν_{41}, CCC bend	**816**	**31**	**ν_{41}, CCC bend**	**817**	**50**	**824**	**144**
ν_{40}, ring def. + C–H bend	834	2	ν_{40}, C–H bend + CH_2 rock	845	3		
ν_{39}, ring def.	852	3	ν_{39}, C–H bend	858	14		
ν_{38}, C–H bend	872	50	ν_{38}, C–H bend + CH_2 rock	890	6		
ν_{37}, CH_2 rock + C–H bend	907	2	ν_{37}, C–H bend	907	1		
ν_{36},	934	1	ν_{36}, C–H bend	927	2		
ν_{35}, C–H bend	949	4	ν_{35}, CCC bend	946	2		
ν_{34},	964	0	ν_{34}, CCC bend	962	0		
ν_{33}, CCC bend	970	1	ν_{33}, CCC bend	975	3		
ν_{32}, CCC and CNC bend	995	3	ν_{32}, C–C stretch	1020	49		
ν_{31}, C–H bend	1025	30	ν_{31}, ring def.	1024	10		
ν_{30}, C–C str.	1082	11	ν_{30}, C–H bend	1078	12		
ν_{29}, C–C str	1091	3	ν_{29}, CH_2 twist	1090	8		
ν_{28}, CH_2 twist + C–H bend	1119	12	ν_{28}, C–H bend	1097	8		
ν_{27}, C–C str	1122	21	ν_{27}, CH_2 wag + C–H bend	1130	8		
ν_{26}, C–H bend	1142	20	ν_{26}, C–H bend	1142	11		
ν_{25}, CH_2 wag + C–H bend	1167	13	ν_{26}, C–H bend	1144	0		
ν_{24}, C–C str	1183	21	ν_{24}, C–C stretch	1184	14		
ν_{23}, C–C str	**1201**	**22**	**ν_{23}, C–H bend**	**1208**	**43**	**1205**	**198**
ν_{22}, C–C str + C–H bend	**1263**	**148**	**ν_{22}, C–H bend**	**1257**	**58**	**1230**	**91**
ν_{21}, C–C str + C–H bend	**1276**	**86**	**ν_{21}, C–H bend**	**1280**	**104**	**1260**	**150**
ν_{20}, C–C str + C–H bend	1291	11	ν_{20}, C–C stretch	1341	8		
ν_{19}, CH_2 scissor + C–C str	1340	29	ν_{19}, CH_2 scissor	1356	44		
ν_{18}, C–C str	1375	17	**ν_{18}, C–C stretch**	**1377**	**140**	**1408**	**164**
ν_{17}, CH_2 scissor	**1383**	**22**	ν_{17}, C–C stretch	1384	20		
ν_{16}, ring 3 C–C str	**1452?**	**17**	**ν_{16}, C–C stretch**	**1440?**	**120**		
ν_{15}, ring 3 C–C str	**1455?**	**9**	**ν_{15}, C–C stretch**	**1454?**	**77**	**1469**	**244**
ν_{14}, rings 1 and 2 C–C str	**1517**	**220**	ν_{14}, C–C stretch	1490	35		
ν_{13}, C–C str	**1583?**	**125**	**ν_{13}, C–C stretch**	**1534**	**126**	**1523**	**164**
ν_{12}, C–C str	**1589?**	**193**	ν_{12}, C–C stretch	1588	2	**1566**	**321**
ν_{11}, ring 3 C–C str	**1612**	**255**	**ν_{11}, ring 3 C–C stretch**	**1614**	**222**	**1584**	**238**
ν_{10}, C=N str	**1762**	**20**	**ν_{10}, C=N stretch**	**1755**	**30**	**1782**	**102**

[a] Possible vibrational band assignments are also shown based on comparison to calculated vibrational frequencies from BPW91/cc-PVDZ computations in the 600–1800 cm^{-1} fingerprint region for the ground singlet state of the two isomers of the azirine intermediates formed from 2-fluorenylnitrene (see text).

8 cm^{-1}). Thus, the spectrum obtained with the 252.7 nm probe wavelength at 15 ns is assigned to the same 2-fluorenylnitrene species observed in the 10 ns, 50 ns, and 100 ns 416 nm probe Raman spectra.

The five Raman bands observed in the 252.7 nm time-resolved resonance Raman spectrum at 10 μs exhibit good agreement with the computed vibrational frequencies for the two dehydroazepine isomer products (within $\approx$7 cm^{-1}, on average, for both **DA1** and **DA2**). The two bands at 1226 cm^{-1} and 1550 cm^{-1} in the 252.7 nm spectrum are close to those observed in the 416 nm spectrum at 5 and 10 μs (1231 and 1550 cm^{-1}, respectively). This is consistent with the same dehydroazepine products being observed in both the 252.7 nm and 416 nm spectra on the microsecond time scale. The relative intensity pattern is different in the 252.7 nm and 416 nm time-resolved resonance Raman spectra of the dehydroazepine isomers. This is attributed to excitation of different electronic transitions.

The 252.7 nm time-resolved resonance Raman spectra in conjunction with the previously reported 416 nm time-resolved resonance Raman spectra indicate that photolysis of 2-azidofluorene first leads to formation of a 2-fluorenylnitrene species (10–100 ns time scale lifetime). The 2-fluorenylnitrene then subsequently forms an azirine intermediate (hundreds of ns time scale lifetime and clearly observed at 500 ns) which, in turn, forms the dehydroazepine ring-expansion products on the microsecond time scale. These time-resolved Raman spectra also provide clear evidence that arylnitrene ring-expansion reactions proceed via an azirine intermediate species to produce the dehydroazepine products in room-temperature solutions. Our results are consistent with and strongly support the predictions by several theoretical

Table 2. Experimental Raman vibrational frequencies observed in the 252.7 nm time-resolved resonance Raman (TR3) spectra of 2-fluorenylnitrene at 15 ns (Figure 1 of this work).[a] The experimental vibrational frequencies are compared to those from UBPW91/cc-PVDZ computations for the singlet 2-fluorenylnitrene (computational results from ref. [60]; see text for more details).

Singlet 2-fluorenylnitrene vibrational mode possible description	UBPW91/cc-PVDZ calcd value [cm^{-1}]	Experiment 252.7 nm and 15 ns TR3 freq. shift [cm^{-1}]	Experiment 416 nm and 10, 50, 100 ns TR3 freq. shift [cm^{-1}]
ν_{51}, ring def.	524		
ν_{50}, CCC bend	563		
ν_{49}, ring def.	567		
ν_{48}, CCC bend	**623**		**637**
ν_{47}, ring def.	690		
ν_{46}, CCC bend	709		
ν_{45}, C–H bend (o.p.)[b]	722		
ν_{44}, CCC bend	738		
ν_{43}, C–H bend	766		
ν_{42}, ring def. + C–H bend	798		
ν_{41}, CCC bend	**814**		**818**
ν_{40}, C–H bend (o.p.)	835		
ν_{39}, C–H bend	850		
ν_{38}, ring def.	885		
ν_{37}, ring def.	907		
ν_{36}, ring def. + C–H bend	934		
ν_{35}, C–H bend (o.p.)	941		
ν_{34}, C–H bend (o.p.)	964		
ν_{33}, CCC bend	980		
ν_{32}, ring 3 C–C stretch	1021		
ν_{31}, C–H bend	1078		
ν_{30}, C–H bend	1102		
ν_{29}, CH_2 twist	1114		
ν_{28}, ring def. + C–H bend	1121		
ν_{27}, ring def. + C–H bend	1141		
ν_{26}, C–H bend + CH_2 wag	1165		
ν_{25}, ring def. + C–H bend	1183		
ν_{24}, ring def. + C–H bend	1202		
ν_{23}, C–C stretch	**1221**	**1226**	
ν_{22}, C–H bend + CH_2 wag	**1276**	**1257**	
ν_{21}, C–C stretch	1296		
ν_{20}, C–C stretch + CH_2 scissor	**1352**		**1331**
ν_{19}, C–C stretch + CH_2 scissor	**1371**		**1367**
ν_{18}, C–C stretch + CH_2 scissor	1377		
ν_{17}, C–C stretch + N–H stretch	**1429**		**1410**
ν_{16}, C–C stretch + C–H_2 scissor	**1431**		
ν_{15}, C–C stretch	**1453**		**1451**
ν_{14}, C–C stretch + C–N stretch	**1475**		**1479**
ν_{13}, C–C stretch	**1495**	**1501**	
ν_{12}, C–C stretch	**1575**	**1544**	**1551**
ν_{11}, C–C stretch + N–H stretch	**1579**	**1568**	**1573**
ν_{10}, C–C stretch	**1604**	**1598**	**1591**

[a] Possible vibrational band assignments are also shown based on comparison to calculated vibrational frequencies from UBPW91/cc-PVDZ computations in the 500–1700 cm^{-1} fingerprint region for the ground singlet and triplet state of 2-fluorenylnitrene (see text). [b] o.p. = out-of-plane

groups that arylnitrene ring-expansion reactions proceed via azirine intermediates to form dehydroazepine species.[42, 64] For example, Karney and Borden[42] used CASSCF and CASPT2N calculations and found the ring-expansion reaction from the $^1A_2$ state of phenylnitrene occurs in two steps via an azirine intermediate (7-azabicyclo[4.1.0]-hept-2,4,6-triene). Similarly, Hadad, Kozankiewicz, and co-workers[64] used B3LYP/6-31G* calculations to study the ring-expansion reactions of perfluorophenyl nitrene and perfluoro-2-napthyl nitrene and also found these proceed via a two-step mechanism to form ketenimimes.

From the time-resolved resonance Raman spectra previously obtained with the 416 nm probe wavelength,[60] we can try to estimate the decay of the 2-fluorenylnitrene to produce the **AZ1** and **AZ2** intermediates and the appearance time of the dehydroazepine products (**DA1** and **DA2**) from decay of the azirine intermediates. Figure 3 plots the intensity of the Raman bands of the 2-fluorenylnitrene species (circles) at 10 ns, 50 ns, 100 ns, and the dehydroazepine species (diamonds) at 1 μs, 5 μs, and 10 μs versus time. A simple exponential decay (or appearance) best fit was made to these data (given by the solid curves in Figure 3). The decay time constant of the 2-fluorenylnitrene (or appearance of the azirine intermediates) was estimated to be ≈40 ns (±15 ns) and the appearance time of the dehydroazepine products was estimated to be ≈6 μs (±3 μs). We note these are rough estimates based only on a few time-delays of the TR^3 spectra. More accurate estimates could be obtained by means of methods, such as time-resolved transient absorption spectroscopy, that are better able to follow the kinetics.

Experimental and theoretical studies of the phenylnitrene ring-expansion reaction indicate the singlet phenylnitrene species (generated by photolysis of phenylazide) has a very short lifetime and quickly proceeds to the dehydroazepine product.[7, 8, 44, 45] This has made it very difficult to experimentally observe the azirine intermediate in this arylnitrene ring-expansion reaction. Spectroscopic studies have established that the dehydroazepine (ketenimine) product is the species trapped by nucleophiles in the phenylnitrene ring-expansion reaction[9, 14, 15] and this is consistent with the lack of experimental observation of the azirine intermediate and its apparent short lifetime. This is in contrast to our present study of the 2-fluorenylnitrene ring-expansion reaction where the azirine intermediate has a relatively long lifetime and is readily observed in the 500 ns 252.7 nm time-resolved Raman spectrum.

We have carried out additional B3LYP/6-31G* calculations to find the relative energies of selected species involved in the singlet 2-fluorenylnitrene ring-expansion reactions involving

0947-6539/03/0906-1382 $ 20.00+.50/0 *Chem. Eur. J.* **2003**, *9*, No. 6

Table 3. Experimental Raman vibrational frequencies observed in the 252.7 nm time-resolved resonance Raman (TR3) spectra of the dehydroazepine product(s) at 10 μs shown in Figure 2.[a] The experimental vibrational frequencies are compared to those from UBPW91/cc-PVDZ computations for the two isomers of the dehydroazepine 2-fluorenyl derivatives (computational results from reference [60]; see text for more details).

Isomer 1 of 2-fluorenyl dehydroazepine		Isomer 2 of 2-fluorenyl dehydroazepine		Experimental freq. shift	
				This work	ref. [60]
vibrational mode possible description	BPW91/cc-PVDZ calcd value [cm^{-1}]	vibrational mode possible description	BPW91/cc-PVDZ calcd value [cm^{-1}]	10 μs TR3 252.7 nm [cm^{-1}]	5 μs TR3 416 nm [cm^{-1}]
ν_{52}, ring def.	503	ν_{51}, ring def.	518		
ν_{51}, ring def. + C=C=N bend	517	ν_{50}, ring def.	552		
ν_{50}, ring def. + C=C=N bend	537	**ν_{49}, ring def. + C=C=N bend**	**565**		**586**
ν_{49}, CCC bend	**591**	ν_{48}, ring def.	617		
ν_{48}, ring def.	621	ν_{47}, ring def.	646		
ν_{47}, ring def.	652	ν_{46}, CCC bend	684		
ν_{46}, ring def.	677	ν_{45}, ring def.	691		
ν_{45}, ring def.	698	**ν_{44}, C–H bend (o.p.)**	**715**	**720**	
ν_{44}, C–H bend (o.p.)[b]	**720**	ν_{43}, CCC bend + C–H bend (o.p.)	748		
ν_{43}, ring def.	728	ν_{42}, C–H bend (o.p.)	760		
ν_{42}, C–H bend (o.p.)	761	**ν_{41}, CCC bend**	**814**		**808**
ν_{41}, CCC bend	**814**	ν_{40}, ring def.	830		
ν_{40}, ring def.	**838**	**ν_{39}, C–H bend (o.p.) + CH_2 rock**	**845**	**844**	
ν_{39}, C–H bend + CH_2 rock	850	ν_{38}, ring def. + CH_2 rock	887		
ν_{38}, ring 1 C–H bend (o.p.)	866	ν_{37}, ring def. + C–H bend	909		
ν_{37}, C–H bend (o.p.) + CH_2 rock	910	ν_{36}, ring def. + C–H bend	925		
ν_{36}, C–H bend (o.p.)	935	ν_{35}, CCC bend	948		
ν_{35}, CCC bend	945	ν_{34}, ring def.	970		
ν_{34}, C–H bend (o.p.)	963				
ν_{33}, C–N str	1000	ν_{33}, CCC bend + C=C–N bend	970		
ν_{32}, ring 3 C–C str	1025	ν_{32}, ring def.	1023		
ν_{31}, ring 1 C–C str	1037	ν_{31}, ring def.	1055		
ν_{30}, ring def. + C–H bend	1085	ν_{30}, ring def. + C–H bend	1088		
ν_{29}, C–C str + C–N str	1099	ν_{29}, ring def. + CH_2 twist	1094		
ν_{28}, CH_2 twist	1120	ν_{28}, C–C stretch	1111		
ν_{27}, C–C str + C–H bend	1133	ν_{27}, C–H bend + CH_2 wag	1124		
ν_{26}, C–H bend	1142	ν_{26}, C–H bend	1142		
ν_{25}, rings 2 and 3 C–C str	1172	ν_{25}, C–H bend	1177		
ν_{24}, CH_2 wag + C–H bend	**1185**	**ν_{24}, C–C str**	**1182**		**1188**
ν_{23}, C–C str	**1228**	**ν_{23}, C–H bend**	**1215**	**1226**	**1231**
ν_{22}, C–C str	**1260**	**ν_{22}, C–C str**	**1260**	**1257**	
ν_{21}, C–H bend	1275	ν_{21}, C–C str + C–H bend	1278		
ν_{20}, ring 1 C–C str	1300	ν_{20}, C–C str	1330		
ν_{19}, C–C str	1334	ν_{19}, CH_2 scissor	1355		
ν_{18}, ring 3 C–C str	1373	ν_{18}, C–C str + C–N str	1372		
ν_{17}, CH_2 scissor	**1390**	**ν_{17}, C–C str**	**1383**		**1407**
ν_{16}, ring 3 C–C str	**1452**	**ν_{16}, C–C str**	**1443**		**1439**
ν_{15}, ring 3 C–C str	**1454**	**ν_{15}, C–C str**	**1452**		**1457**
ν_{14}, C–C str rings 1 and 2	1548	ν_{14}, C–C str	1512		
ν_{13}, C–C str	**1570**	**$\tilde{\nu}_{13}$, C–C str**	**1556**	**1550**	**1560**
ν_{12}, C–C str	**1588**	**ν_{12}, C–C str**	**1587**	**1598**	
ν_{11}, C–C str ring 3	**1611**	**ν_{11}, C–C str ring 3**	**1612**		**1608**
ν_{10}, N=C=C asym. str	1887	ν_{10}, N=C=C asym. str	1891		

[a] Possible vibrational band assignments are also shown based on comparison to calculated vibrational frequencies from BPW91/cc-PVDZ computations in the 500–1700 cm^{-1} fingerprint region for the ground singlet state of the two isomers of the dehydroazepine products (see text). [b] o.p. = out-of-plane.

AZ1 and **AZ2** azirines to form **DA1** and **DA2** dehydroazepine products and these results are depicted in Figure 4. Inspection of Figure 4 shows that the transition states (**TS1** and **TS2**) leading from the 2-fluorenylnitrene species to the two azirines **AZ1** and **AZ2** have very similar energies within ≈0.2 kcal mol^{-1} of each other. This predicts that both **AZ1** and **AZ2** intermediates will be produced in significant amounts from the singlet 2-fluorenylnitrene species. This is in agreement with the comparison of the experimental TR[3] spectra and computed vibrational frequencies and intensities that indicate both **AZ1** and **AZ2** species both contribute noticeably to the 500 ns TR[3] spectrum of the azirine species. The barriers to reaction for the azirines **AZ1** and **AZ2** to go on to their dehydroazepine products **DA1** and **DA2** are similar with the barrier being somewhat higher for the formation of the **DA2** product. This suggests that both **DA1** and **DA2** products would be formed with **DA1** being somewhat more prevalent than **DA2**.

Interestingly, the stronger iminocyclohexadienyl character of singlet 2-fluorenylnitrene relative to triplet 2-fluorenylnitrene leads to a noticeably smaller singlet–triplet gap of ≈7.4 kcal mol^{-1} (from UBPW91/cc-PVDZ) compared to ≈18 kcal mol^{-1} for the singlet–triplet gap of the phenylnitrenes.[60] This smaller singlet–triplet splitting in the 2-fluorenylnitrene system could be caused by its larger conjugation system and greater charge delocalization into the phenyl ring

  0947-6539/03/0906-1383 $ 20.00+.50/0

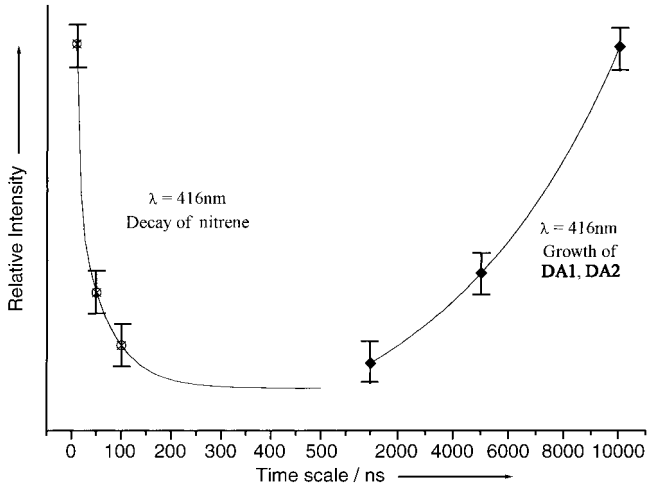

Figure 3. Plot of the intensity of the Raman bands from the 416 nm TR3 spectra of reference [60] for the 2-fluorenylnitrene species (○) at 10 ns, 50 ns, 100 ns and the dehydroazepine species (◆) at 1 μs, 5 μs, and 10 μs versus time. A simple exponential decay (or appearance) best fit was made to these data and is displayed as a solid line.

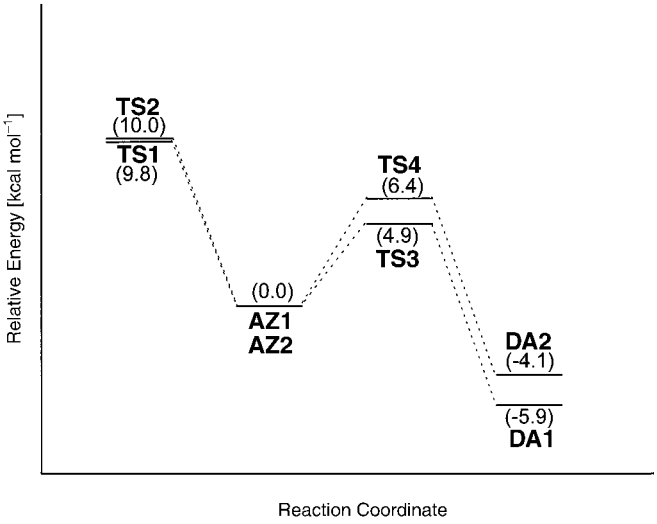

Figure 4. The relative energies [kcal mol^{-1}] of selected species participating in the singlet 2-fluorenylnitrene ring-expansion reactions involving **AZ1** and **AZ2** azirines to form **DA1** and **DA2** dehydroazepine products obtained from B3LYP/6–31G* calculations.

compared to the phenylnitrene system. This suggests the singlet 2-fluorenylnitrene species may become more stable relative to the transition state to form the azirine species (**AZ1** and **AZ2**). This hypothesis is consistent with the significantly longer lifetime of the 2-fluorenylnitrene species in the 416 nm TR^3 spectra (10–100 ns)[60] compared to the singlet phenylnitrene (<1 ns).[7, 8, 44, 45] The greater iminocyclohexadienyl character of the singlet 2-fluorenylnitrene also appears to lead to longer C–C bond lengths adjacent to the C=N bond. This could conceivably help relieve some of the ring strain of the azirine three-membered ring and substantially stabilize the azirine intermediate. This could be consistent with our time-resolved resonance Raman experimental observation of a relatively long-lived azirine intermediate in the 2-fluorenylnitrene ring-expansion reaction to produce dehydroazepine products. The iminocyclohexadienyl character of the 2-fluorenylnitrene and their azirine intermediates affects both the C–C bonds of the phenyl ring and the C–N bond and appears to affect the relative stability of these species in the ring-expansion reaction to make dehydroazepines. This suggests that the ability of the *para*-phenyl substituent to influence or change the iminocyclohexadienyl character of the phenylnitrene moiety may be responsible for the longer lived 2-fluorenylnitrene and azirine intermediates. If this is actually the case, then we would predict that different *para*-phenyl ring derivatives with differing degrees of iminocyclohexadienyl character would lead to noticeable differences and some correlation with the lifetimes of the singlet arylnitrene and its azirine intermediates. The related *para*-phenyl-substituted phenylnitrenium ion derivatives display varying iminocyclohexadienyl character with the degree following the order: 2-fluorenylnitrenium ion > 4-biphenylylnitrenium ion > *N*-(4-biphenylyl)-*N*-methylnitrenium ion, as determined from previous time-resolved vibrational and density functional studies.[56, 61, 62] If the *para*-phenyl-substituted singlet arylnitrene derivatives display similar trends, then we would expect the lifetimes of the singlet arylnitrenes and their azirine intermediates to follow a similar trend with the longer lifetimes correlated with larger iminocyclohexadienyl character of the *para*-phenyl-substituted arylnitrene. Further experimental and theoretical work is needed to ascertain if this is actually the case and to better understand how a *para*-phenyl substituent effects influence the arylnitrene ring-expansion reactions.

The relatively long-lived nitrene and azirine intermediate(s) observed in the 2-fluorenylnitrene ring-expansion reaction provide a valuable opportunity to explore the chemical reactivity of these types of species with various substrates. It has been difficult to trap or directly probe the structure of the azirine intermediate in the phenylnitrene and other arylnitrene ring-expansion reactions in room-temperature solutions, and only the trapping of several azirines formed from substituted phenylnitrenes have been reported.[19, 65, 66] Aryl azirine intermediates are similar to 2H-azirines, which are highly reactive and useful compounds for many synthetic reactions and can function as either an electrophile or as a nucleophile.[67–73] Time-resolved vibrational (Raman or IR) and absorption spectroscopies should prove useful to examine the reactions of various substrates with the arylnitrene and arylazirine intermediates to produce further intermediates or products. Such studies are planned and will enable the chemical reactivity of *para*-substituted arylnitrenes and arylazirines to be more fully explored.

Conclusion

Time-resolved resonance Raman spectra of photoproducts formed from ultraviolet photolysis of 2-azidofluorene in acetonitrile solution were obtained with a 252.7 nm probe wavelength. Different Raman spectra were observed at delay times of 15 ns, 500 ns, and 10 μs. The Raman vibrational frequencies were compared to those predicted by density functional calculations for probable photoproduct species.

0947-6539/03/0906-1384 $ 20.00+.50/0 *Chem. Eur. J.* **2003**, *9*, No. 6

The 15 ns, 500 ns, and 10 μs Raman band frequencies agreed reasonably well for those of 2-fluorenylnitrene, the two isomers of azirine formed from 2-fluorenylnitrene, and the two dehydroazepine products, respectively. The Raman band frequencies observed in the 15 ns and 10 μs spectra were also consistent with those observed in previous time-resolved resonance Raman experiments with a 416 nm probe wavelength.[60] The 252.7 nm and 416 nm time-resolved resonance Raman spectra indicate that photolysis of 2-azidofluorene first produces 2-fluorenylnitrene then forms a relatively long-lived azirine intermediate (observed at 500 ns with the 252.7 nm probe wavelength) that then forms dehydroazepine ring-expansion products seen on the microsecond time scale. Our results indicate that arylnitrenes produce dehydroazepine ring-expansion products via azirine intermediates in room-temperature solutions, and this supports the reaction mechanism proposed by several theoretical groups.[42, 64]

Comparison of the 2-fluorenylnitrene ring-expansion with several other arylnitrenes suggest that substitution of another phenyl ring *para* to the nitrene in phenylnitrenes significantly alters the stability and lifetimes of the intermediates so that the arylnitrenes and azirines can have noticeably longer lifetimes. The chemical reactions and reactivity of these interesting arylnitrene and azirine intermediates can, therefore, be more easily explored by means of trapping experiments.

Experimental Section and Computational Methods

Synthesis of the azide precursor, **2-azidofluorene**: 2-Azidofluorene was made based on a literature method for making azido compounds.[74] We employed the same procedure and characterization of the synthesized compound as previously detailed in reference [60]. The reader is referred to those for a detailed description of the synthetic procedure.

Caution: The azide precursor compound, 2-azidofluorene, is potentially explosive (more likely if allowed to dry) and should be handled with care.

Computational methods: The Gaussian 98 W set of programs[75] were used for all of the density functional calculations reported here. Complete geometry optimization and vibrational frequency calculations were carried out analytically by means of the BPW91 method[76, 77] and the cc-PVDZ basis set[78] for the two azirine intermediates that can be formed from 2-fluorenylnitrene (**AZ1** and **AZ2**). The computed geometry parameters and vibrational frequencies for the two azirine intermediates (**AZ1** and **AZ2** formed from 2-fluorenylnitrene) from selected parts of the Gaussian output files are given in the Supporting Information. The optimized geometry for the two transitions states (**TS1** and **TS2**) forming the two azirine intermediates from 2-fluorenylnitrene, the two azirine intermediates (**AZ1** and **AZ2**, respectively), the two transition states (TS3 and TS4) for the ring-expansion reaction, and the ring-expansion products (**DA1** and **DA2**, respectively) were found from B3LYP/6-31G* calculations and are given in Figure 4.

Time-resolved resonance Raman spectroscopy experiments: The 2-azidofluorene parent compound was prepared with concentrations in the 2–5 mM range in acetonitrile solvent for the time-resolved resonance Raman experiments. The time-resolved resonance Raman experimental apparatus and methods have been detailed in previous publications, so only a short description will be given here.[60–62, 79–83] The harmonics of two nanosecond-pulsed Nd:YAG lasers and their hydrogen Raman-shifted laser lines supplied the pump (266 nm) and probe (252.7 nm) excitation wavelengths were used in the time-resolved resonance Raman experiments. A pulse delay generator (Stanford Research Systems model DG-535) was used to electronically synchronize the two Nd:YAG lasers with respect to each other and to control their relative timing (monitored by two fast photodiodes whose output was shown on a 500-MHz oscilloscope). The pump and probe pulses had a jitter of < 5 ns. A near-collinear geometry was used to softly focus the two laser beams onto a flowing liquid jet of the sample. Reflective optics and a backscattering geometry were used to collect the Raman scattered light and image it through a polarization scrambler mounted on the entrance slit of a 0.5-m spectrograph. The spectrograph grating then dispersed the Raman scattered light onto a liquid nitrogen-cooled CCD detector that accumulated the Raman signal for $\approx 300-600$ s before being read out to an interfaced PC computer. Approximately 10–20 of these readouts were added together to obtain a resonance Raman spectrum and pump-only, probe-only, and pump–probe resonance Raman spectra. The known Raman bands from the acetonitrile solvent were employed to calibrate the wavenumber shifts of the resonance Raman spectra. The time-resolved resonance Raman spectrum was obtained by subtracting the probe-only spectrum from the pump–probe spectrum to delete the solvent and parent Raman bands and then the pump-only spectrum and the background spectrum were also subtracted from the pump–probe spectrum.

Acknowledgement

This work was supported by grants from the Committee on Research and Conference Grants (CRCG), the Research Grants Council (RGC) of Hong Kong (HKU 7112/00P), and the Large Items of Equipment Allocation 1993–1994 from the University of Hong Kong.

[1] E. F. V. Scriven, in *Reactive Intermediates*, *Vol. 2* (Ed.: R. A. Abramovich), Plenum, New York, **1982**, Chapt. 1.
[2] C. Wentrup, *Reactive Molecules*, Wiley-Interscience, New York, **1984**, Chapt. 4.
[3] M. S. Platz, in *Azides and Nitrenes: Reactivity and Utility* (Ed.: E. F. V. Scriven), Academic, New York, **1984**, Chapt. 7.
[4] M. S. Platz, V. M. Maloney, in *Kinetics and Spectroscopy of Carbenes and Biradicals* (Ed.: M. S. Platz), Plenum, New York, **1990**, pp. 303–320.
[5] M. S. Platz, E. Leyva, K. Haider, *Org. Photochem.* **1991**, *11*, 367.
[6] G. B. Schuster, M. S. Platz, *Adv. Photochem.* **1992**, *17*, 69–143.
[7] M. S. Platz, *Acc. Chem. Res.* **1995**, *28*, 487–492.
[8] W. T. Borden, N. P. Gritsan, C. M. Hadad, W. L. Karney, C. R. Kemnitz, M. S. Platz, *Acc. Chem. Res.* **2000**, *33*, 765–771.
[9] A. K. Schrock, G. B. Schuster, *J. Am. Chem. Soc.***1984**, *106*, 5228–5234.
[10] T. Donnelly, I. R. Dunkin, D. S. D. Norwood, A. Prentice, C. J. Shields, P. C. P. Thomson, *J. Chem. Soc. Perkin Trans. 2* **1985**, 307–310.
[11] I. R. Dunkin, T. Donnelly, T. S. Lockhart, *Tetrahedron Lett.* **1985**, *26*, 359–362.
[12] E. Leyva, M. S. Platz, *Tetrahedron Lett.* **1985**, *26*, 2147–2150.
[13] E. Leyva, M. S. Platz, G. Persy, J. Wirz, *J. Am. Chem. Soc.* **1986**, *108*, 3783–3790.
[14] C. J. Shields, D. R. Chrisope, G. B. Schuster, A. J. Dixon, M. Poliakoff, J. J. Turner, *J. Am. Chem. Soc.* **1987**, *109*, 4723–4726.
[15] Y.-Z. Li, J. P. Kirby, M. W. George, M. Poliakoff, G. B. Schuster, *J. Am. Chem. Soc.* **1988**, *110*, 8092–8098.
[16] R. Poe, J. Grayzar, M. J. T. Young, E. Leyva, K. Schnapp, M. S. Platz, *J. Am. Chem. Soc.* **1991**, *113*, 3209–3211.
[17] M. J. T. Young, M. S. Platz, *J. Org. Chem.* **1991**, *56*, 6403–6406.
[18] R. Poe, K. Schnapp, M. J. T. Young, J. Grayzar, M. S. Platz, *J. Am. Chem. Soc.* **1992**, *114*, 5054–5067.
[19] C. G. Younger, R. A. Bell, *J. Chem. Soc. Chem. Commun.* **1992**, 1359–1361.
[20] S.-J. Kim, T. P. Hamilton, H. F. Schaefer, *J. Am. Chem. Soc.* **1992**, *114*, 5349–5355.
[21] D. A. Hrovat, E. E. Waali, W. T. Borden, *J. Am. Chem. Soc.* **1992**, *114*, 8698–8699.
[22] A. Marcinek, M. S. Platz, *J. Phys. Chem.* **1993**, *97*, 12674–12677.
[23] A. Marcinek, E. Leyva, D. Whitt, M. S. Platz, *J. Am. Chem. Soc.* **1993**, *115*, 8609–8612.
[24] K. A. Schnapp, R. Poe, E. Leyva, N. Soundarajan, M. S. Platz, *Bioconjugate Chem.* **1993**, *4*, 172–177.

  0947-6539/03/0906-1385 $ 20.00+.50/0

[25] K. A. Schnapp, M. S. Platz, *Bioconjugate Chem.* **1993**, *4*, 178 – 183.
[26] G. B. Anderson, D. E. Falvey, *J. Am. Chem. Soc.* **1993**, *115*, 9870 – 9871.
[27] T. Ohana, M. Kaise, S. Nimura, O. Kikuchi, A. Yabe, *Chem. Lett.* **1993**, 765 – 768.
[28] P. A. Davidse, M. J. Kahley, R. A. McClelland, M. Novak, *J. Am. Chem. Soc.* **1994**, *116*, 4513 – 4514.
[29] A. Marcinek, M. S. Platz, Y. S. Chan, R. Floresca, K. Rajagopalan, M. Golinski, D. Watt, *J. Phys. Chem.* **1994**, *98*, 412 – 419.
[30] K. Lamara, A. D. Redhouse, R. K. Smalley, J. R. Thompson, *Tetrahedron* **1994**, *50*, 5515 – 5526.
[31] R. A. McClelland, P. A. Davidse, G. Haczialic, *J. Am. Chem. Soc.* **1995**, *117*, 4173 – 4174.
[32] R. J. Robbins, L. L.-N. Yang, G. B. Anderson, D. E. Falvey, *J. Am. Chem. Soc.* **1995**, *117*, 6544 – 6552.
[33] S. Srivastava, D. E. Falvey, *J. Am. Chem. Soc.* **1995**, *117*, 10186 – 10193.
[34] R. A. McClelland, M. J. Kahley, P. A. Davidse, *J. Phys. Org. Chem.* **1996**, *9*, 355 – 360.
[35] R. A. McClelland, M. J. Kahley, P. A. Davidse, G. Hadzialic, *J. Am. Chem. Soc.* **1996**, *118*, 4794 – 4803.
[36] R. J. Robbins, D. M. Laman, D. E. Falvey, *J. Am. Chem. Soc.* **1996**, *118*, 8127 – 8135.
[37] R. J. Moran, D. E. Falvey, *J. Am. Chem. Soc.* **1996**, *118*, 8965 – 8966.
[38] J. Morawietz, W. Sander, *J. Org. Chem.* **1996**, *61*, 4351 – 4354.
[39] O. Castell, V. M. Garcia, C. Bo, R. Caballol, *J. Comput. Chem.* **1996**, *17*, 42 – 48
[40] J. Michalak, H. B. Zhai, M. S. Platz, *J. Phys. Chem.* **1996**, *100*, 14028 – 14036.
[41] X.-Z. Sun, I. G. Virrels, M. W. George, H. Tomioka, *Chem. Lett.* **1996**, 1089 – 1090.
[42] W. L. Karney, W. T. Borden, *J. Am. Chem. Soc.* **1997**, *119*, 1378 – 1387.
[43] W. L. Karney, W. T. Borden, *J. Am. Chem. Soc.* **1997**, *119*, 3347 – 3350.
[44] N. P. Gritsan, T. Yuzawa, M. S. Platz, *J. Am. Chem. Soc.* **1997**, *119*, 5059 – 5060.
[45] R. Born, C. Burda, P. Senn, J. Wirz, *J. Am. Chem. Soc.* **1997**, *119*, 5061 – 5062.
[46] N. P. Gritsan, H. B. Zhai, T. Yuzawa, D. Karweik, J. Brooke, M. S. Platz, *J. Phys. Chem. A* **1997**, *101*, 2833 – 2840.
[47] R. J. Moran, D. E. Falvey, *J. Am. Chem. Soc.* **1996**, *118*, 8965 – 8966.
[48] S. Srivastava, J. P. Toscano, R. J. Moran, D. E. Falvey, *J. Am. Chem. Soc.* **1997**, *119*, 11552 – 11553.
[49] E. Leyva, R. Sagredo, *Tetrahedron* **1998**, *54*, 7367 – 7374.
[50] A. Nicolaides, H. Tomioka, S. Murata, *J. Am. Chem. Soc.* **1998**, *120*, 11530 – 11531.
[51] A. Nicolaides, T. Naakayama, K. Yamazaki, H. Tomioka, S. Koseki, L. L. Stracener, R. J. McMahon, *J. Am. Chem. Soc.* **1999**, *121*, 10563 – 10572.
[52] N. P. Gritsan, Z. Zhu, C. M. Hadad, M. S. Platz, *J. Am. Chem. Soc.* **1999**, *121*, 1202 – 1207.
[53] N. P. Gritsan, A. Gudmundsdottir, D. Tigelaar, M. S. Platz, *J. Phys. Chem. A* **1999**, *103*, 3458 – 3461.
[54] N. P. Gritsan, D. Tigelaar, M. S. Platz, *J. Phys. Chem. A* **1999**, *103*, 4465 – 4469.
[55] M. Cerro-Lopez, N. P. Gritsan, Z. Zhu, M. S. Platz, *J. Phys. Chem. A* **2000**, *104*, 9681 – 9686.
[56] S. Srivastava, P. H. Ruane, J. P. Toscano, M. B. Sullivan, C. J. Cramer, D. Chiapperino, E. C. Reed, D. E. Falvey, *J. Am. Chem. Soc.* **2000**, *122*, 8271 – 8278.
[57] N. P. Gritsan, I. Likhotvorik, M.-L. Tsao, N. Celebi, M. S. Platz, W. L. Karney, C. R. Kemnitz, W. T. Borden, *J. Am. Chem. Soc.* **2001**, *123*, 1425 – 1433.
[58] H. Inui, S. Murata, *Chem. Lett.* **2001**, 832 – 833.
[59] A. Nicolaides, T. Enyo, D. Miura, H. Tomioka, *J. Am. Chem. Soc.* **2001**, *123*, 2628 – 2636.
[60] S. Y. Ong, P. Zhu, Y. F. Poon, K. H. Leung, W.-H. Fang, D. L. Phillips, *Chem. Eur. J.* **2002**, *8*, 2163 – 2171.
[61] P. Zhu, S. Y. Ong, P. Y. Chan, K. H. Leung, D. L. Phillips, *J. Am. Chem. Soc.* **2001**, *123*, 2645 – 2649.
[62] P. Zhu, S. Y. Ong, P. Y. Chan, Y. F. Poon, K. H. Leung, D. L. Phillips, *Chem. Eur. J.* **2001**, *7*, 4928 – 4936.
[63] I. R. Dunkin, P. C. P. Thomson, *J. Chem. Soc. Chem. Commun.* **1980**, 499 – 501.
[64] B. Kozankiewicz, I. Deperasiñska, H. B. Zhai, Z. Zhu, C. M. Hadad, *J. Phys. Chem. A* **1999**, 103, 5003 – 5010.
[65] S. E. Carrol, B. Nay, E. F. V. Scriven, H. Suschitzky, D. R. Thomas, *Tetrahedron Lett.* **1977**, 3175-.
[66] P. E. Nielsen, O. Buchardt, *Photochem. Photobiol.* **1982**, 35, 317 – 323.
[67] A. Padwa, A. D. Woolhouse in *Comprehensive Heterocyclic Chemistry* (Eds.: A. R. Katritzky, C. W. Rees), Pergamon Press, Oxford, **1984**.
[68] V. Nair in *Heterocyclic Compounds, Vol. 42*, (Ed.: A. Hassner), Wiley, New York, **1983**, Part I, pp. 215 – 332.
[69] G. L'Abbé, P. Van Stappen, J. P. Dererk, *J. Chem. Soc. Chem. Commun.* **1982**, 784 – 785.
[70] G. L'Abbé, P. Van Stappen, S. Toppet, G. Germain, G. Scheefer, *Bull. Soc. Chim. Belg.* **1983**, *92*, 193 – 194.
[71] M. J. Alves, T. L. Gilchrist, J. H. Sousa, *J. Chem. Soc. Perkin Trans. 1* **1999**, 1305 – 1310.
[72] T. L. Gilchrist, R. Mendonca, *Synlett* **2000**, 1843 – 1845.
[73] T. M. V. D. Pinho e Melo, C. S. J. Lopes, A. M. d'A. Rocha Gonsalves, A. M. Beja, J. A. Paixão, M. R. Silva, L. A. da Vega, *J. Org. Chem.* **2002**, 67, 66 – 71.
[74] a) B. R. Brown, L. W. Yielding, W. E. White, Jr., *Mutat. Res.* **1980**, *70*, 17 – 27; b) W. E. White, Jr., L. W. Yielding, In *Methods in Enzymology, Vol. XLVI Affinity Labeling* (Eds.: W. B. Jakoby, M. Wilchek), Academic Press, Inc., Orlando, Florida, **1977**, pp. 646 – 647.
[75] M. J. Frisch, G. W. Trucks, H. B. Schlegel, G. E. Scuseria, M. A. Robb, J. R. Cheeseman, V. G. Zakrzewski, J. A. Montgomery, Jr., R. E. Stratmann, J. C. Burant, S. Dapprich, J. M. Millam, A. D. Daniels, K. N. Kudin, M. C. Strain, O. Farkas, J. Tomasi, V. Barone, M. Cossi, R. Cammi, B. Mennucci, C. Pomelli, C. Adamo, S. Clifford, J. Ochterski, G. A. Petersson, P. Y. Ayala, Q. Cui, K. Morokuma, D. K. Malick, A. D. Rabuck, K. Raghavachari, J. B. Foresman, J. Cioslowski, J. V. Ortiz, A. G. Baboul, B. B. Stefanov, G. Liu, A. Liashenko, P. Piskorz, I. Komaromi, R. Gomperts, R. L. Martin, D. J. Fox, T. Keith, M. A. Al-Laham, C. Y. Peng, A. Nanayakkara, C. Gonzalez, M. Challacombe, P. M. W. Gill, B. Johnson, W. Chen, M. W. Wong, J. L. Andres, C. Gonzalez, M. Head-Gordon, E. S. Replogle, J. A. Pople, J. A. Gaussian, Inc., Pittsburgh PA, **1998**.
[76] A. Becke, *J. Chem. Phys.* **1986**, *84*, 4524 – 4529.
[77] J. P. Perdew, K. Burke, Y. Wang, *Phys. Rev. B* **1996**, *54*, 16533 – 16539.
[78] T. H. Dunning, *J. Chem. Phys.* **1989**, *90*, 1007 – 1023.
[79] D. Pan, D. L. Phillips, *J. Phys. Chem. A* **1999**, *103*, 4737 – 4743.
[80] X. Zheng, D. L. Phillips, *J. Phys. Chem. A* **2000**, *104*, 6880 – 6886.
[81] X. Zheng, C. W. Lee, Y.-L. Li, W.-H. Fang, D. L. Phillips, *J. Chem. Phys.* **2001**, *114*, 8347 – 8356.
[82] Y.-L. Li, K. H. Leung, D. L. Phillips, *J. Phys. Chem. A* **2001**, 105, 10621 – 10625.
[83] Y.-L. Li, D. M. Chen, D. Wang, D. L. Phillips, *J. Org. Chem.* **2002**, 67, 4228 – 4235.

Received: April 30, 2002
Revised November 26, 2002 [F4054]

  0947-6539/03/0906-1386 $ 20.00+.50/0